



**A new probe for detecting zinc-bound carbonic anhydrase in cell lysates and cells**

Journal:	<i>ChemComm</i>
Manuscript ID	CC-COM-03-2018-002034.R2
Article Type:	Communication

SCHOLARONE™  
Manuscripts



Journal Name

COMMUNICATION

## A new probe for detecting zinc-bound carbonic anhydrase in cell lysates and cells

Received 00th January 20xx,  
Accepted 00th January 20xx

Radhika Mehta,<sup>a</sup> Munaum H. Qureshi,<sup>a</sup> Meredith K. Purchal,<sup>a</sup> Sylvester M. Greer,<sup>a</sup> Shanzhong Gong,<sup>b</sup> Chinh Ngo,<sup>a</sup> Emily L. Que\*<sup>a</sup>

DOI: 10.1039/x0xx00000x

www.rsc.org/

**We report the synthesis and application of a small molecule probe for carbonic anhydrase (CA) to track *holo*-CA in cell lysates and live-cell models of zinc dyshomeostasis. The probe displays a 12-fold increase in fluorescence upon binding to bovine CA and also responds to human CA isoforms.**

The human genome encodes up to a million proteins. Nearly 30% of these are metalloproteins<sup>1</sup> and ~10% contain zinc as the metal co-factor.<sup>2</sup> These proteins serve structural and catalytic roles and vary in concentration and structure, with specific isoforms localized to different organelle, cell and tissue types.<sup>3-5</sup> In the cell, metalloproteins exist in both active *holo* (metalated) and inactive *apo* (metal-free) states<sup>6</sup> that are dictated by the available buffered metal ion concentration and/or the presence of an appropriate metallochaperone.<sup>6-8</sup> Further, perturbation of normal metal homeostasis can affect cellular metalloprotein status in terms of expression, metalation status, activity, and localization.<sup>9,10</sup>

While many fluorescent probes have been reported for mapping intracellular levels of labile (loosely-bound) zinc<sup>11-13</sup> there are limited tools available for live-cell tracking of zinc tightly bound to metalloproteins.<sup>14-21</sup> Traditional immunostaining methods and fluorescent-protein labelling fail to provide metalation state information. Thus, small molecule fluorophores that can reversibly bind *holo* metalloproteins represent a promising avenue for monitoring these protein-metal complexes in cellular contexts.<sup>22,23</sup>

In the present study, we synthesized a selective, small molecule fluorophore to map the intracellular localization of the active, metalated form carbonic anhydrase (CA)<sup>24</sup> and implemented this probe in cell lysate protein analysis and in a cellular model of zinc dyshomeostasis. CA is a zinc-based lyase that catalyzes the reversible conversion of water and carbon

dioxide to a bicarbonate ion and proton. The active site of this enzyme contains zinc coordinated to three histidines (His) and a water or hydroxide ion in a distorted tetrahedral geometry.<sup>24,25</sup> There are 15 different isoforms of CA that occur in the cell.<sup>26</sup> Recent work highlights the importance of the presence of specific zinc transporters (ZnTs) in governing the metalation status and activity of this enzyme, highlighting a link between CA activity and cellular zinc homeostasis.<sup>9,10</sup>

To make a fluorophore specific for CA, we incorporated a sulfonamide moiety that has a high binding affinity for the Zn<sup>2+</sup> active site of CA.<sup>27</sup> The sulfonamide is linked to N,N-dimethylaminophthalimide (DMAP)<sup>28</sup> that is non-fluorescent in aqueous environments and fluorescent in hydrophobic environments, such as that of the CA active site (Fig. 1). From a synthetic perspective, this fluorophore scaffold can be readily modified with different groups, facilitating the production of control compounds as well as probes with modified binding properties. While others have reported probes for cellular CA,<sup>17-21</sup> we introduce new avenues for applications of this class of dyes for tracking metalated CA in native protein gels of cell lysates and in live cell imaging. We further demonstrate how perturbing the amount of available cellular zinc affects both CA-based fluorescence as well as fluorescence from the free zinc probe FluoZin-3 (FZ3).

Our small molecule probe targeted at *holo* CA was readily

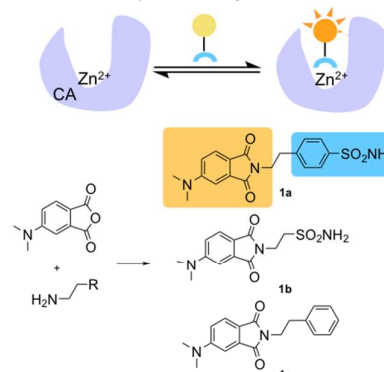


Figure 1. Fluorescence 'turn-on' and reaction scheme for carbonic anhydrase-targeted molecules **1a-c** in this work.

<sup>a</sup> Department of Chemistry, University of Texas at Austin, 105 E 24th St Stop A5300, Austin, TX 78712.

<sup>b</sup> Department of Molecular Biosciences, University of Texas at Austin, 2506 Speedway, Austin, TX 78712.

Electronic Supplementary Information (ESI) available: [details of any supplementary information available should be included here]. See DOI: 10.1039/x0xx00000x

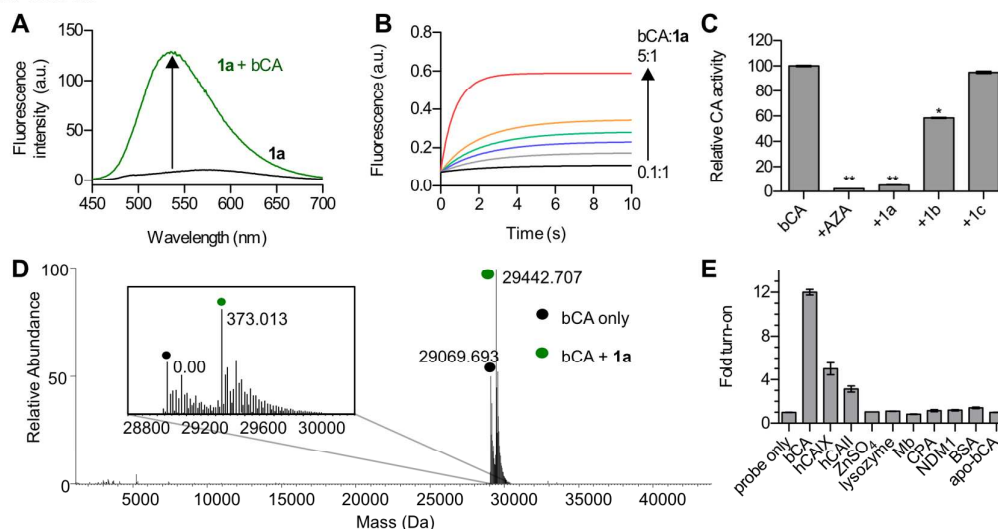


Figure 2. (A) Fluorescence spectra of probe **1a** (5  $\mu\text{M}$ ) in the absence (black) and presence of 1 equiv bCA (green) in HEPES buffer (pH 7.2) at room temperature.  $\lambda_{\text{ex}} = 420 \text{ nm}$ . (B) Kinetics of binding between **1a** (1  $\mu\text{M}$ ) and CA were studied *via* stopped-flow by measuring fluorescence with variable concentrations of CA (0.1, 0.3, 0.5, 0.7, 1 and 5  $\mu\text{M}$ ). (C) NPA hydrolysis showing relative CA activity (2  $\mu\text{M}$  bCA) upon incubation with the probes (2  $\mu\text{M}$ ) and NPA (250  $\mu\text{M}$ ) monitored at  $\lambda_{\text{obs}} = 400 \text{ nm}$ . Paired t-test was performed with bCA vs the probes (5%). (D) High resolution mass spectra (MS) for bCA and ligand **1a** showing the deconvoluted MS. The inset displays an expanded region of the deconvoluted MS from 28,800 Da to 30,000 Da showing the mass shift corresponding to **1a**. (E) Fluorescence fold turn-on of probe **1a** with bCA, hCAIX, hCAII, ZnSO<sub>4</sub>, lysozyme, myoglobin (Mb), carboxypeptidase A (CPA), New Delhi- $\beta$ -lactamase 1 (NDM1) bovine serum albumin (BSA), and apo-bCA. All measurements, except with CPA, were performed in HEPES buffer at room temperature. Studies with CPA were conducted in 50 mM Tris buffer, pH 8.0.

synthesized from known precursors (Supporting information). DMAP<sup>28-30</sup> was coupled to 4-(2-aminoethyl)benzene sulfonamide in refluxing acetic acid to give CA-targeted probe **1a** in 33% yield (Fig. 1; ESI<sup>†</sup>). Further, two control compounds, **1b** and **1c**, were synthesized to test the importance of the aryl and sulfonamide moieties for interactions with CA. The spectroscopic properties of **1a-c** are tabulated in Table S1<sup>†</sup>. All three fluorophores displayed the expected solvatochromism,<sup>29, 31, 32</sup> with a bathochromic shift in absorbance and fluorescence upon switching from non-polar to polar solvents.

Following incubation with bovine carbonic anhydrase (bCA), **1a** (1:1 ratio) displayed a 12-fold increase in fluorescence and a shift in  $\lambda_{\text{em}}$  from 575 nm to 533 nm (Fig. 2A). Probe **1b** only displayed a 3-fold fluorescence increase and a shift in  $\lambda_{\text{em}}$  from 580 nm to 540 nm (Fig. S2<sup>†</sup>). Fluorescence increases observed upon addition of protein are consistent with interaction of these probes with the more hydrophobic environment of the bCA active site.<sup>14, 33</sup> The decreased response of **1b** relative to **1a** illustrates the importance of aryl interactions with the hydrophobic portion of the binding pocket.<sup>34</sup> Importantly, native mass spectrometry (Orbitrap) of a 1:1 mixture of bCA and **1a** demonstrated the formation of a bCA-**1a** complex (Fig. 2D, S3<sup>†</sup>), suggesting strong interactions between these species.

The importance of the interaction of sulfonamide binding group with zinc in the active site was tested by a number of control studies. No increase in fluorescence was observed when probe **1c** was incubated with bCA (Fig. S2<sup>†</sup>). Interactions between **1a** and CA is selective for when Zn<sup>2+</sup> is bound to the active site. Incubation of **1a** with apo bCA<sup>16</sup> or a solution of ZnSO<sub>4</sub> produced no fluorescence increase (Fig. 2E) supporting the theory of **1a** interaction with the *holo*-enzyme only. Further, **1a** displays no fluorescence increase upon addition of other metalated forms of CA (Co<sup>2+</sup>-CA, Ni<sup>2+</sup>-CA, Cd<sup>2+</sup>-CA; Figure S5<sup>†</sup>). Moreover, we tested the CA activity in the presence of probes **1a-c** using the NPA (4-nitrophenylacetate) hydrolysis assay.<sup>34</sup> We observed a large decrease in relative CA activity

(Fig. 2C) upon addition of **1a** (down to 5%), comparable to known CA inhibitor acetazolamide, AZA (2%). AZA is known to bind strongly to the zinc center in the enzyme active site with a  $K_i$  of 12 nM and 25 nM with human CA (hCA) isoforms namely hCAII and hCAIX respectively.<sup>35, 36</sup> In contrast, 58% of CA activity was retained with **1b** signifying weaker binding of the probe with CA, consistent with the observed fluorescence response (Fig. S2<sup>†</sup>). As expected, most of the enzymatic activity was retained with **1c** (95%). Incubation of **1a** with other proteins including lysozyme and bovine serum albumin as well as metalloproteins myoglobin, carboxypeptidase A, and New Delhi metallo- $\beta$ -lactamase 1 resulted in no fluorescence turn-on (Fig. 2E). In addition to bCA, we tested our probe with hCAII and hCAIX, resulting in 3-fold and 5-fold turn-on responses respectively (Fig. 2E). The  $K_{\text{off}}$ ,  $k_{\text{on}}$ , and  $K_d$  of **1a**-bCA binding were analyzed using stopped-flow fluorescence measurements (Fig. 2B, S4<sup>†</sup>) and were calculated to be  $0.145 \text{ s}^{-1}$ ,  $0.241 \mu\text{M}^{-1}\text{s}^{-1}$  and  $0.64 \mu\text{M}$  respectively. These values lie well within the range reported for benzene sulfonamides with CA and are consistent with a micromolar binding interaction between probe and protein.<sup>37</sup>

Selectivity and in-gel fluorescence<sup>38</sup> of **1a** with CA was tested using an adapted native-SDS polyacrylamide gel electrophoresis protocol<sup>39</sup> (native-SDS PAGE, Fig. 3) that allowed us to keep the proteins in their native state and obtain more spatially distinct bands compared to simple native PAGE. The interaction of the probe **1a** with CA was followed *via* native-SDS gel in a defined mixture of proteins and in bovine red blood cell lysates.<sup>40, 41</sup> As shown in Fig. 3A, lanes 2 and 3 containing bCA and **1a** have fluorescent bands following UV illumination (254 nm). Coomassie staining in Fig. 3B confirms these bands correspond to the ones observed for bCA only (Lane 1), which indicates no change in retention factor of the protein in the presence of probe. Fluorescent bands observed in the wells at the top of the lanes doped with **1a** come from free probe. Probe **1a** was also incubated with Biorad IEF protein standard (Lane 5) that includes 5 metalloproteins *viz.* hemoglobin (Hb), myoglobin (Mb), bCA, hCA and cytochrome C

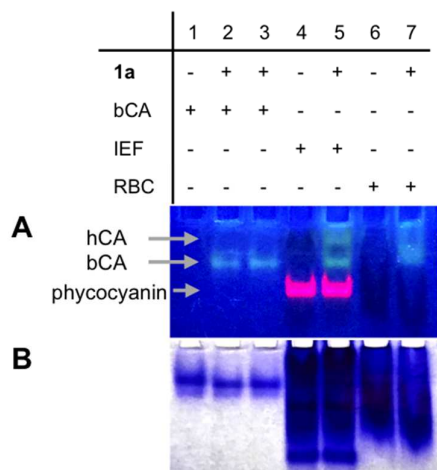


Figure 3. Native-SDS PAGE (A) In-gel fluorescence (UV excitation) with **1a** and CA in RBC lysates, IEF protein mixture (containing Hb, Mb, bCA, hCA, cytochrome C, BSA, lentil lectin, phycocyanin and lactoglobulin B), and bCA showing fluorescent bands in the gel corresponding to bCA and hCA only. (B) Coomassie staining of the same gel showing presence of proteins in all lanes. The gel was run at 180V, 4°C for 30 mins on a 7.5% Mini-Protean TGX gel. The protein concentrations were bCA (10 µg), Biorad IEF standard (5 µL of 16 mg/mL), bovine RBC lysate (20 µL of 20 mg/mL) with excess probe **1a**.

along with bovine serum albumin (BSA), lentil lectin, phycocyanin and lactoglobulin B (9 proteins total). As expected, with the IEF protein mixture, only the bands corresponding to bCA and hCA display fluorescence with probe **1a**, demonstrating the selectivity of **1a** in targeting only CA in a mixture of proteins. We note that the pink fluorescence belongs to phycocyanin, which is a pigment-protein complex from the light-harvesting phycobiliprotein family.<sup>42</sup>

Importantly, we demonstrate the ability to selectively track CA in native cell lysates from bovine red blood cells (ESI<sup>+</sup>). Post-lysis and ethanol-chloroform extractions to remove excess hemoglobin,<sup>40</sup> the remaining protein mixture is expected to contain some hemoglobin, CA, catalase and redox proteins.<sup>43,44</sup> The bovine RBC lysates incubated with **1a** in Lane 7 displayed fluorescence in the region corresponding to CA (Fig. 3A) and not with other proteins present (Fig. 3B). This validated the selectivity and applicability of **1a** as a suitable, selective fluorophore for CA in complex protein mixtures.

We next used **1a** to image the intracellular zinc-bound CA and correlate this with free zinc levels using zinc specific fluorophore, FluoZin3 to study the effect of free zinc perturbations on CA. HeLa cells were treated with **1a** (1 µM) to label CA while commercially available FluoZin3-AM ester (2.5 µM), which converts to FluoZin3 (FZ3) intracellularly upon esterase cleavage, was used to label intracellular free zinc ions. Due to emission overlap between the two probes, **1a** and FluoZin3-AM were incubated in different cell samples under identical conditions (ESI<sup>+</sup>). Following incubation with probe **1a**, cells were treated with (i) AZA, a strong CA inhibitor or (ii) N,N,N',N'-tetrakis(2-pyridinylmethyl)-1,2-ethanediamine (TPEN), a heavy metal chelator with a  $K_d$  for  $Zn^{2+}$  of  $10^{-16}$  M or (iii) Zinc pyrithione (ZnPT), a zinc ionophore.<sup>45</sup> (Fig. 4).

Cells treated with AZA (10 µM) displayed a significant decrease in **1a** fluorescence in HeLa (Fig. 4A) and HEK 293 cells (Fig. S7<sup>†</sup>). Parallel *in vitro* fluorescence studies showed that incubation of AZA to the bCA-**1a** complex in buffer does result in a significant decrease (66%) in intensity over an hour (Fig. S6<sup>†</sup>). Conversely, FZ3 fluorescence showed no decrease upon treatment. This demonstrates that AZA primarily decreases fluorescence of the CA-bound zinc pool with minimal effect on labile zinc fluorescence. Incubation with TPEN (10 µM) showed no decrease in intensity (Fig. 4B) for **1a** while a major loss in fluorescence was observed with FZ3. This large decrease in FZ3 is as expected and has been previously reported in multiple cell types.<sup>11, 46-48</sup> *In vitro* studies (Fig. S6<sup>†</sup>) with TPEN added to **1a**-bCA mixtures failed to change the fluorescence supporting the observed effects in the cellular context. This points to the fact that while free zinc levels are affected by TPEN treatment, the CA-bound zinc levels remain the same over this short period of time. Treatment with the ionophore ZnPT (1 µM) increases the intracellular free zinc.<sup>46, 47, 49</sup> and as expected, a 3-fold increase in FZ3 fluorescence was observed within 5 minutes of incubation. The fluorescence with **1a**, however, remained the same both in cells and *in vitro* (Fig. S6<sup>†</sup>).

To the best of our knowledge, this is the first study that reports the effects of different treatments on the free zinc and

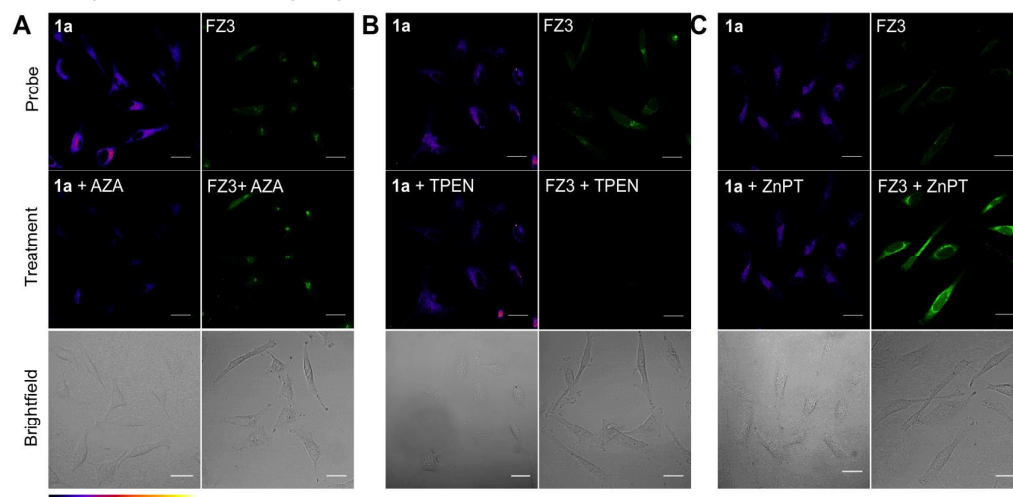


Figure 4. Confocal images taken in live-cell imaging media at 37°C showing fluorescence response with **1a** (1 µM;  $\lambda_{ex}$ : 405 nm,  $\lambda_{em}$ : 505-565 nm) and FZ3 (2.5 µM;  $\lambda_{ex}$ : 488 nm,  $\lambda_{em}$ : 505-565 nm) incubated in HeLa cells. Following dye incubation, cells were subjected to (A) AZA treatment (10 µM, 25 min) and (B) TPEN treatment (10 µM, 15 min) and (C) ZnPT treatment (1 µM, 5 min) respectively. Scale bars: 30 µm.

CA-bound zinc levels. These results suggest that there is a notable effect of zinc perturbations on the free Zn<sup>2+</sup> levels while the CA-bound zinc is unaffected under reported concentrations and timescales. Future work will expand on these studies. The ability to track metalloproteins in this way has the potential to provide valuable insight into cellular metal homeostasis and these studies serve as an initial step towards understanding how metal ion pools in the cell interact and are perturbed in the presence of metal chelators and ionophores.

We thank Profs. Jennifer S. Brodbelt and Kenneth A. Johnson for helpful discussions and Prof. Joseph P. Emerson and Prof. Walter Fast for providing hCAII and NDM1 respectively. We thank the ICMB imaging facility for help and training on the confocal microscope. We acknowledge the following funding sources: Start-up funds (ELQ) and an undergraduate research fellowship (MKP) from the University of Texas (ELQ), NSF (Grant CHE1402753 to JSB) and the Welch Foundation (Grant F-1155 to JSB, Grant F-1883 to ELQ). SMG acknowledges a graduate fellowship from the American Chemical Society Division of Analytical Sciences.

### Conflicts of interest

There are no conflicts to declare.

### Notes and references

1. A. Sussulini and J.S. Becker, *Metalomics* 2011, **3**, 1271.
2. C. Andreini, L. Banci, I. Bertini and A. Rosato, *J Prot Res* 2006, **5**, 196.
3. A. Aspatwar, M.E. Tolvanen and S. Parkkila, *BMC Mol Biol* 2010, **11**, 25.
4. W. Maret, *Metalomics* 2010, **2**, 117.
5. K.J. Waldron, J. Rutherford, D. Ford, and N.J. Robinson, *Nature* 2009, **460**, 823.
6. A.W. Foster, D. Osman, and N.J. Robinson, *J Biol Chem* 2014, **289**, 28095.
7. T.V. O'Halloran and V.C. Culotta *J Biol Chem* 2000, **275**, 25057.
8. A.C. Rosenzweig, *Chem Biol* 2002, **9**, 673.
9. T. Tsuji, Y. Kurokawa, J. Chiche, J. Pouysségur, H. Sato, H. Fukuzawa, M. Nagao and T. Kambe, *J Biol Chem* 2017, **292**, 2159.
10. N.H. McCormick and S.L. Kelleher, *Am J Physiol Cell Physiol* 2012, **303**, C291.
11. Huang, and S.J. Lippard, *Methods Enzymol* 2012, **505**, 445.
12. D.W. Domaille, E.L. Queand C.J. Chang, *Nat Chem Biol* 2008, **4**, 168.
13. E.L. Que, R. Bleher, F.E. Duncan, B.Y. Kong, S.C. Gleber, S. Vogt, S. Chen, S.A. Garwin, A.R. Bayer, V.P. Dravid, T.K. Woodruff and T.V. O'Halloran, *Nat Chem* 2015, **7**, 130.
14. W.T. Yu, T.W. Wu, C.L. Huang, I.C. Chen and K.T. Tan, *Chem Sci* 2016, **7**, 301.
15. C.L. Fleming, T.D. Ashton, C. Nowell, M. Devlin, A. Natoli, J. Schreuders and F.M. Pfeffer, *Chem Comm* 2015, **51**, 7827.
16. R.B. Thompson, W.O. Whetsell, B.P. Maliwal, C.A. Fierke and C.J. Frederickson, *J Neurosci Methods* 2000, **96**, 35.
17. V. Alterio, R.M. Vitale, S.M. Monti, C. Pedone, A. Scozzafava, A. Cecchi, G. De Simone and C.T. Supuran, *J Am Chem Soc* 2006, **128**, 8329.
18. C.J. Carroux, G.M. Rankin, J. Moeker, L.F. Bornaghi, K. Katneni, J. Morizzi, S.A. Charman, D. Vullo, C.T. Supuran, and S.A. Poulsen, *J Med Chem* 2013, **56**, 9623.
19. C.C. Wykoff, N.J. Beasley, P.H. Watson, K.J. Turner, J. Pastorek, A. Sibtain, G.D. Wilson, H. Turley, K.L. Talks, P.H. Maxwell, C.W. Pugh, P.J. Ratcliffe and A.L. Harris, *Cancer Res* 2000, **60**, 7075.
20. T.K. Hurst, D. Wang, R.B. Thompson and C.A. Fierke, *Biochim Biophys Acta* 2010, **1804**, 393.
21. C.A. Fierke and R.B. Thompson, *Biomaterials* 2001, **14**, 205.
22. L. Dubois, K. Douma, C.T. Supuran, R.K. Chiu, M.A. van Zandvoort, S. Pastoreková, A. Scozzafava, B.G. Wouters and P. Lambin, *Radiother Oncol* 2007, **83**, 367.
23. K. Teruya, K.F. Tonissen and S.A. Poulsen, *MedChemComm* 2016, **7**, 2045.
24. V.M. Krishnamurthy, G.K. Kaufman, A.R. Urbach, I. Gitlin, K.L. Gudiksen, D.B. Weibel and G.M. Whitesides, *Chem Rev* 2008, **108**, 946.
25. H. Vahrenkamp, *Dalton Trans* 2007, **42**, 4751.
26. V. Alterio, A. Di Fiore, K. D'Ambrosio, C.T. Supuran and G. De Simone, *Chemical Reviews* 2012, **112**, 4421.
27. C.T. Supuran, *Bioorg Med Chem Letters* 2010, **20**, 3467.
28. M. Sainlos, and B. Imperiali, *Nat Protoc* 2007, **2**, 3219.
29. G. Loving and B. Imperiali, *J Am Chem Soc* 2008, **130**, 13630.
30. M. Sainlos, W.S. Iskenderian and B. Imperiali, *J Am Chem Soc* 2009, **131**, 6680.
31. X. Liu, Q. Qiao, W. Tian, W. Liu, J. Chen, M.J. Lang and Z. Xu, *J Am Chem Soc* 2016, **138**, 6960.
32. M.E. Vázquez, J.B. Blanco and B. Imperiali, *J Am Chem Soc* 2005, **127**, 1300.
33. Y.D. Zhuang, P.Y. Chiang, C.W. Wang and K.T. Tan, *Angew Chem Int Ed Engl* 2013, **52**, 8124.
34. R.F. Chen and J.C. Kernohan, *J Biol Chem* 1967, **242**, 5813.
35. D. Vullo, M. Franchi, E. Gallori, J. Pastorek, A. Scozzafava, S. Pastorekova and C.T. Supuran, *Bioorg Med Chem Letters* 2003, **13**, 1005.
36. A. Di Fiore, S.M. Monti, M. Hilvo, S. Parkkila, V. Romano, A. Scaloni, C. Pedone, A. Scozzafava, C.T. Supuran and G. De Simone, *Proteins: Structure, Function, and Bioinformatics* 2009, **74**, 164.
37. T.H. Maren, *Mol Pharmacol* 1992, **41**, 419.
38. M.T. Morgan, P. Bagchi, and C.J. Fahrni, *J Am Chem Soc* 2011, **133**, 15906.
39. A.B. Nowakowski, W.J. Wobig and D.H. Petering, *Metalomics* 2014, **6**, 1068.
40. J. da Costa Ores, L. Sala, G.P. Cerveira and S.J. Kalil, *Chemosphere* 2012, **88**, 255.
41. E.E. Rickli, S.A. Ghazanfar, B.H. Gibbons and J.T. Edsall, *J Biol Chem* 1964, **239**, 1065.
42. N.T. Eriksen, *Appl Microbiol Biotechnol* 2008, **80**, 1.
43. F. Talamo, C. D'Ambrosio, S. Arena, P. Del Vecchio, L. Ledda, G. Zehender, L. Ferrara, A. Scaloni, *Proteomics* 2003, **3**, 440.
44. P. Walicke, S. Varon and M. Manthorpe, *J Neurosci* 1986, **6**, 1114.
45. K. Golovine, R. G. Uzzo, P. Makhov, P.L. Crispin, D. Kunkle and V.M. Kolenko, *The Prostate* 2008, **68**, 1443.
46. Y. Qin, J.G. Miranda, C.I. Stoddard, K.M. Dean, D.F. Galati and A.E. Palmer, *ACS Chem Biol* 2013, **8**, 2366.
47. P.J. Dittmer, J.G. Miranda, J.A. Gorski and A.E. Palmer, *J Biol Chem* 2009, **284**, 16289.
48. Y. Qin, P.J. Dittmer, J.G. Park, K.B. Jansen and A.E. Palmer, *Proc Natl Acad Sci U S A* 2011, **108**, 7351.
49. Y. Chen, B. Lai, Z. Zhang and S.M. Cohen, *Metalomics* 2017, **9**, 250.